

A BIOMETRIC IDENTIFICATION SYSTEM BASED ON THYROID TISSUE ECHO-MORPHOLOGY *

José C. R. Seabra

Instituto de Sistemas e Robótica, Instituto Superior Técnico, Av. Rovisco Pais, Torre Norte 6º piso, 1049-001 Lisboa, Portugal

Ana L. N. Fred

Instituto de Telecomunicações, Instituto Superior Técnico, Av. Rovisco Pais, Torre Norte 10º piso, 1049-001 Lisboa, Portugal

Keywords: Biometrics, Thyroid gland, Ultrasound, Acoustic impedance, Texture, Diagnosis.

Abstract: This paper proposes a biometric system based on features extracted from the thyroid tissue accessed through 2D ultrasound. Tissue echo-morphology, which accounts for the intensity (echogenicity), texture and structure has started to be used as a relevant parameter in a clinical setting. In this paper, features related to texture, morphology and tissue reflectivity are extracted from the ultrasound images and the most discriminant ones are selected as an input for a prototype biometric identification system. Several classifiers were tested, with the best results (90% identification rate) being achieved with the maximum a posteriori classifier. Another classifier which only takes into account the reflectivity parameter achieved a reasonable identification rate of 70%. This suggests that the acoustic impedance (reflectivity) of the tissue is a good parameter to discriminate between individuals. This paper shows the effectiveness of the proposed classification, which can be used not only as a new biometric modality but also as a diagnostic tool.

1 INTRODUCTION

The thyroid is one of the largest endocrine glands in the body (see Fig. 1). It controls how quickly the body burns energy, makes proteins and how sensitive the body should be to other hormones (Tor00). Thyroid ultrasonography is a non-invasive diagnostic exam, which provides immediate information on the structure and the characteristics of thyroid glands. This imaging modality is widely used in clinical practice because it combines low cost, short acquisition time, absence of ionizing radiations and sensitivity in ascertaining the morphology of the thyroid gland, as well as the size and number of thyroid nodules.

The ultrasound images usually present a low *signal to noise ratio* (SNR) and are characterized by a type of multiplicative noise called *speckle* that accompanies all coherent imaging modalities. It appears when images are obtained by using coherent radiation and is the result of the constructive and destructive interference of the echoes scattered from heterogeneous tissues and organs (AT79).

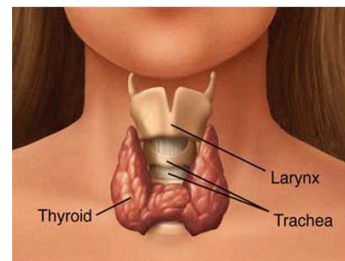


Figure 1: Anatomy of the thyroid gland.

The characteristic granular speckle pattern present in the ultrasound images makes the diagnostic task harder, whereas the subjectivity involved in their interpretation can be regarded as their major drawback. A framework which could provide explicit features extracted from the images would lead to a more reliable medical diagnosis, providing the experts with a second opinion and reducing the misdiagnosis rates.

Some studies have been developed which aim at characterizing the thyroid tissue using ultrasound image processing and analysis. Image intensity information has been used for the identification of thyroid Hashimoto disease (MBSE86), for the detection of

*Partially supported by FCT, under ISR/IST plurianual funding

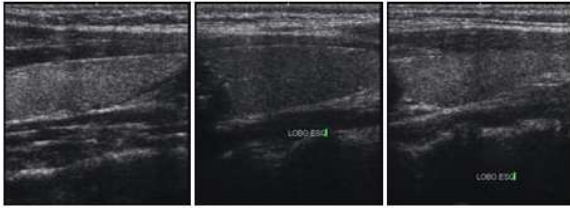


Figure 2: Examples of thyroid ultrasound images, presenting different echo-morphologies. a) Hyperechogenic, b) Hypoechoic and c) Heterogeneous thyroids.

nodular thyroid lesions, and for thyroid tumor classification. Textural image information encoded by means of co-occurrence matrix features (HDS73) have been used for identification of chronic inflammations of the thyroid gland (SSST03b; SSST03a) and for the discrimination between normal and pathologic tissues (CMAL06).

Tissue echo-morphology, which accounts for the intensity (echogenicity), texture and structure, has started to be used as a relevant parameter in a clinical setting (see Fig.2). Basically, features extracted from a given region, tissue or organ can be used to identify (classify) a patient as normal or as suffering from a pathological condition. In a classification context, this is considered to be a two-class problem.

This paper proposes a biometric system based on features extracted from the thyroid tissue accessed through 2D ultrasound. Biometrics deals with identification of individuals based on their biological or behavioral characteristics. Identification (Who am I?) refers to the problem of establishing a subject's identity - either from a set of already known identities (closed identification problem) or otherwise (open identification problem) (PKM⁺07).

Thyroid tissue echo-morphology qualify to be a biometric because it is a universal feature, which means that every person has the characteristic, is distinct from one individual to another, is permanent and can be easily collected through a common ultrasound scanner.

The paper is organized as follows. Section 2 formulates the problem and section 3 describes the feature module used in the biometric system. Section 4 presents the classifiers used in the identification problem. Section 5 presents the results obtained by the biometric system and section 6 concludes the paper.

2 PROBLEM FORMULATION

In this paper, an analogy between two problems is made. In the context of medical diagnosis, a subject is assigned to one of two classes N (normal) or P (patho-

logical). The risk of classifying pathological patients as normal (false negatives) should be penalized. Regarding a biometric identification problem, there is a class assigned to each individual. The maximum likelihood probabilities (or other types of scores) are computed in order to label the individual with its corresponding class.

The problem addressed in this paper can be stated as follows: given C_i classes, each corresponding to a different individual (registered in the database), and O_i observations, corresponding to 2D ultrasound sample images of the thyroid tissue recorded from each individual, establish the identity of new observations (label to the corresponding classes), which is a typical Human identification problem

The diagram block of the biometric system used in this paper is illustrated in Fig.3. It is mainly composed of three modules: (i) the sensor module, (ii) the feature extraction module, and (iii) the classification module.

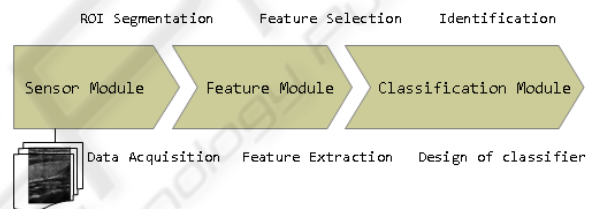


Figure 3: Diagram block of the biometric identification system.

The sensor module accounts for image acquisition. Ultrasound images of the thyroid gland were acquired longitudinally and transversally to the neck of 10 individuals, using a ultrasound scanner (Siemens Sonoline G50) operating in brightness (B-) mode. For each individual, the two lobes of the thyroid were scanned and 2 images per lobe were acquired. All thyroids were scanned under the same operating conditions in order to make the echo-morphological features extracted from the images independent on the scanner properties.

3 FEATURE MODULE

The feature module is an important part of the biometric system because it determines which features are used for identification. In this section it is also important to consider how the thyroid glands are segmented from the ultrasound images, which features qualify for individual characterization, and from those features which of them are more relevant for discriminating between classes (subjects).

3.1 Segmentation

Before extracting the relevant features which describe the echo-morphology of the thyroid glands it is important to segment its anatomy from the ultrasound images. This is a step that should be take into account in order to develop an automatic and robust biometric tool.

The thyroid glands are the regions of interest from where the features could be extracted. This can be done by manually outline the contours of the thyroid, which is incredibly tedious and time-consuming.

One way to circumvent this problem is to use automatic or semi-automatic methods (Active Contours (XP98), Level Sets (vBSVN02), Graph Cuts (BVZ01; KZ04)). In this paper, a semi-automatic method based on Gradient Vector Flow (GVF) active contours (snakes) is used.

Active contours, or snakes, are computer-generated curves that move within images to find the boundaries of the region of interest. The GVF snake begins with the calculation of a field of forces, called the GVF forces, over the image domain. The GVF forces are used to drive the snake, modeled as a physical object having a resistance to both stretching and bending towards the boundaries of the object. The GVF forces are calculated by applying generalized diffusion equations to both components of the gradient of an image edge map (see Fig.4). The semi-automatic nature of the segmentation process is due to user-dependent initialization: in fact, to make the method more robust, the user should provide a rough initialization of the contour by giving some initial clicks on the image.

3.2 Feature Extraction

After obtaining the segmented thyroid glands, 6 rectangular windows (32 by 32 pixels) were extracted from each lobe (see Fig.5). Three different types of features are then computed for each rectangular window: (i) the rayleigh parameter, (ii) 3 wavelet energy coefficients, (iii) 4 radon transform parameters. These features are also combined with the longitudinal mid-distance measure for each thyroid gland. This distance corresponds to the vertical distance measured between the borders of the thyroid at its middle section.

3.3 Rayleigh Parameter

The speckle pattern present in the ultrasound images is a result of the interference of echoes at the surface

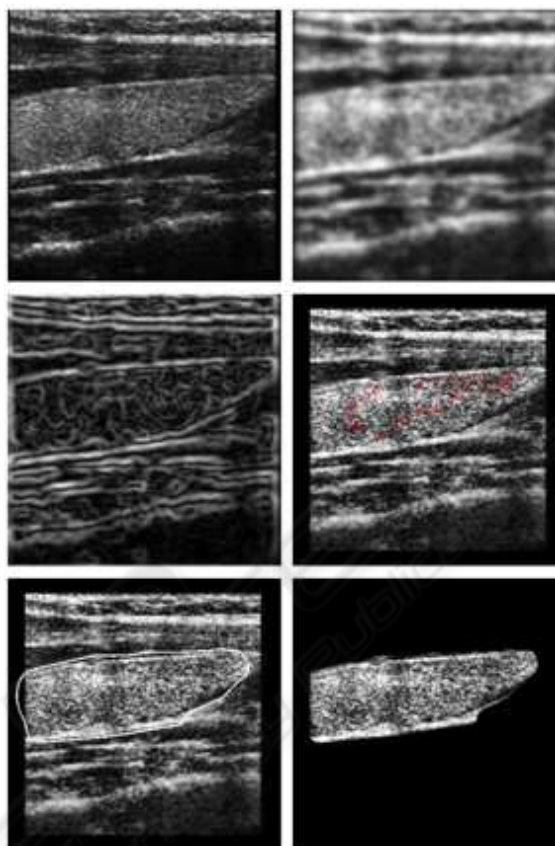


Figure 4: Semi-automatic segmentation using GVF active contours (from top left to bottom right): (i) original image, (ii) image convolved with gaussian mask, (iii) image edge map, (iv) initialization, (v) final contour, (vi) segmented thyroid.

of the transducer, which emanate from the acoustic impedance of the tissues.

Several statistical models are proposed in the literature to describe this kind of pattern (MT06). One of the most used in ultrasound (US), LASER and *Synthetic Aperture Radar* (SAR) is the Rayleigh distribution (Bur78). Commonly the speckle pattern is called speckle noise, and is often studied in de-noising problems. Another view of the problem, which is considered in this paper, is to accurately reconstruct the ultrasound images to provide a measure of the local acoustic impedance of the tissues.

In this context, a bayesian reconstruction method with a log-Euclidean prior is used (SXS08). In this approach, the ill-posedness nature of the reconstruction (de-noising) problem is circumvented by using *a priori* information about the unknown image to be estimated. The estimation is formulated as an optimization task where a two-term energy function is minimized. The first term pushes the solution toward the observations and the second regularizes the solution.

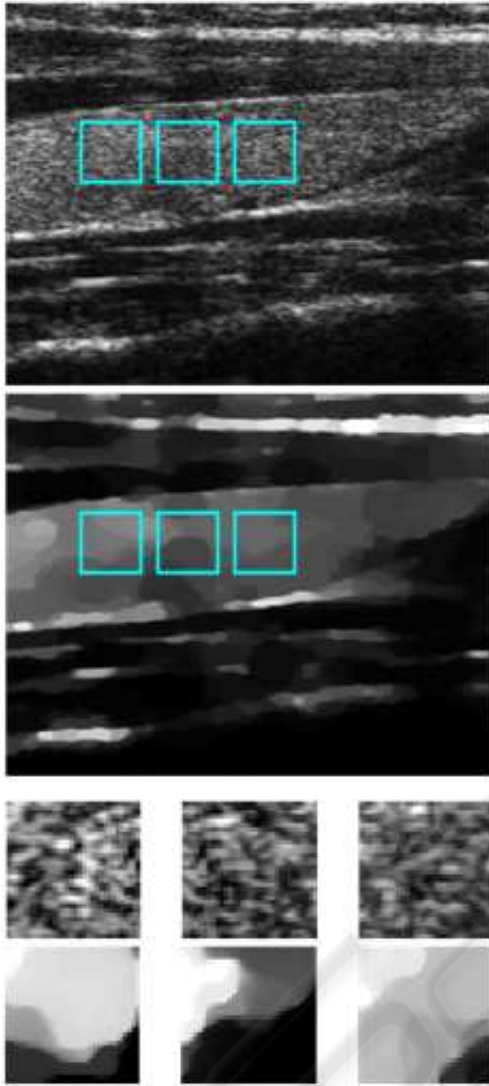


Figure 5: (i) Original image, (ii) reconstructed image (local rayleigh parameters), and (iii) rectangular windows are extracted from each thyroid lobe.

The reconstruction procedure is formulated as the optimization of a convex function and a Newton method is adopted to obtain the minimizer (BV04). This strategy guarantees a convergence to the global minimum in a small number of iterations.

Let $X = \{x_{i,j}\}$ and $Y = \{y_{i,j}\}$ be a $N \times M$ image presenting the acoustic impedance of the tissue and a speckle image, respectively. The *speckle* pattern of the image $Y = \{y_{i,j}\}$ is described by a Rayleigh distribution,

$$p(y_{i,j}|x_{i,j}) = \frac{y_{i,j}}{x_{i,j}^2} e^{-\frac{y_{i,j}}{x_{i,j}}}. \quad (1)$$

The estimation of X from Y is formulated as the

following optimization task

$$\hat{X} = \underset{X}{\operatorname{arg\,min}} E(X, Y), \quad (2)$$

where $E(X, Y)$ is an energy function.

The optimization problem, described by equation (2), is usually *ill-posed* in the Hadamard sense. This difficulty may be overcome by using the *maximum a posteriori* (MAP) criterion,

$$E(X, Y) = \underbrace{E_Y(X, Y)}_{\text{data fidelity term}} + \underbrace{E_X(X)}_{\text{prior term}}, \quad (3)$$

where $E_Y(X, Y)$, called *data fidelity term*, is the symmetric of the log-likelihood function

$$E_Y(X, Y) = -\log \left[\prod_{i,j=1}^{N,M} p(y_{i,j}|x_{i,j}) \right], \quad (4)$$

where it is assumed statistical independence of the observations (DSL98).

The energy function to be minimized is given by

$$E(F, Y) = \sum_{i,j} \left[\frac{y_{i,j}^2}{2} e^{-f_{i,j}} + f_{i,j} \right] \quad (5)$$

$$+ \alpha \sum_{i,j} \sqrt{(f_{i,j} - f_{i-1,j})^2 + (f_{i,j} - f_{i,j-1})^2} + \epsilon.$$

The solution is an image (see Fig.5 (ii) and (iii)), in which the value of each pixel is the Rayleigh parameter that characterizes accurately the local reflectivity of the tissue being scanned.

3.4 Wavelet Energy Coefficients

Texture information is hypothesized as being a relevant parameter to discriminate between thyroids and therefore individuals. One way to assess the texture of a thyroid image is to decompose it using 2D wavelets (see Fig.6).

This kind of decomposition consists in using low and high pass filters onto the approximation coefficients at level j (the original image) in order to obtain the approximation at level $j+1$, and the details in three orientations (horizontal, vertical, and diagonal). This method is performed along 3 levels. Every subimage contains information of a specific scale and orientation, which is conveniently separated. Spatial information is retained within the subimages. The amount of detail for each resolution level, which accounts for the level of heterogeneity in the thyroid gland, is computed as the sum of horizontal, vertical and diagonal detail energies for each level. Therefore, multi-resolution measures of heterogeneity are used as inputs for the biometric identification system.

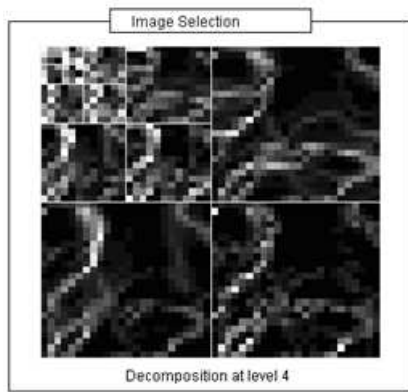


Figure 6: Wavelet decomposition. Multi-resolution texture is assessed through the detail energy levels.

3.5 Radon Transform Features

In this paper, it is also hypothesized that the thyroid tissue may be characterized by different directionality patterns observed in the ultrasound images. The encoding of the directional patterns is realized by means of Radon Transform features (SIDM07). The idea is to project the image intensity along a radial line oriented at different angles (0, 45, 90 and 135 degrees).

Let (x, y) be the cartesian coordinates of a point in a 2D image, and $u(x, y)$ the image intensity. Then, the 2D radon transform denoted as $R_u(\rho, \theta)$ is given by

$$R_u(\rho, \theta) = \int_{-\infty}^{+\infty} \int_{-\infty}^{+\infty} u(x, y) \delta(\rho - x \cos \theta - y \sin \theta) dx dy$$

where ρ is the perpendicular distance of a line from the origin and θ is the angle formed by the distance vector. The feature vector can be defined as

$$F = [\sigma([R_{u_1}(\rho, \theta_1) \dots, R_{u_n}(\rho, \theta_1)]), \sigma([R_{u_1}(\rho, \theta_2) \dots, R_{u_n}(\rho, \theta_2)]), \dots, \sigma([R_{u_1}(\rho, \theta_p) \dots, R_{u_n}(\rho, \theta_p)])], \quad (6)$$

where $\sigma()$ accounts for the contribution of the radon transform along a given angle $\theta_i = \{0, 45, 90, 135^\circ\}$.

3.6 Dimensionality Reduction

At this point, 9 features per sample (each sample corresponding to a rectangular window) were extracted: 1 Rayleigh parameter, 1 mid-distance measure, 3 wavelet energies, and 4 radon transform parameters. The amount of features extracted (9 features per sample, 6 samples per thyroid lobe, 2 lobes per individ-

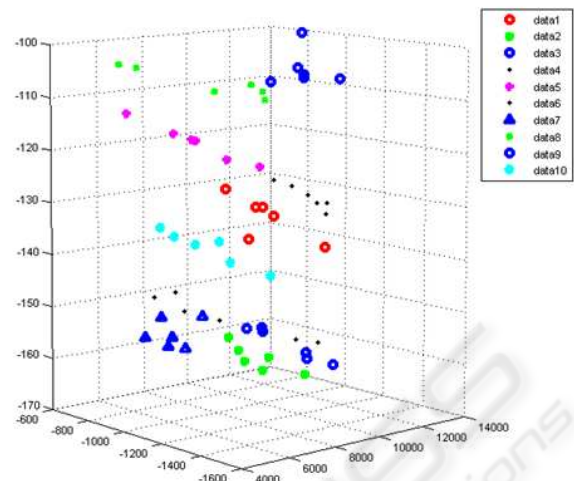


Figure 7: Representation of the observations (6 samples per individual) in the new PCA-derived feature space.

ual, 10 individuals) makes the identification problem a complex task.

One way to deal with this problem and to eliminate the redundancy among features is to use principal component analysis (PCA). This approach is used to better handle and visualize the data by selecting the 3 most discriminating axis in the feature space and computing the 3 most relevant features (projection of the observations onto these axis). In summary, 3 features (components of the PCA) per observation sample are used in the identification problem. Fig.7 shows the representation of the observations (each individual sample) in the new feature space, where the 3 components of the PCA represent the 3 dimensions of the plot.

This new PCA-derived feature space can be projected onto a 2 dimensional feature space. Fig.8 shows that the 2D features are able to clearly discriminate between two classes of individuals: one class addressed to men and the other to women. Even though no prior information is known about the clinical status of the individuals subject to this test it is clearly suggested that textural information might be correlated with the different types and quantities of hormones produced by men and women. This fact can lead to thyroids presenting different acoustic impedances and textures. This also explains the good discrimination between male and female populations.

At this point, we can suggest that this system might be useful as a soft biometric system for gender identification.

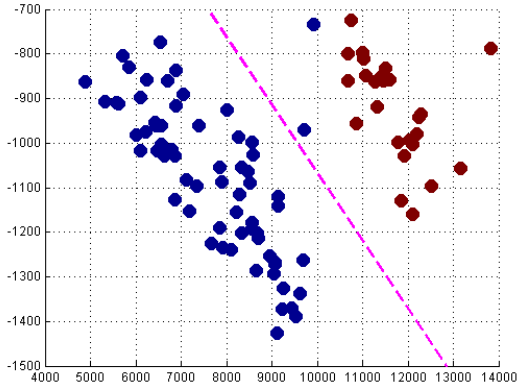


Figure 8: 2D feature space, showing a clear discrimination of the observed samples into two classes (types of subjects).

4 CLASSIFICATION MODULE

In this paper, a closed set identification problem is addressed, which means that N possible outputs are generated for N possible models. The decision on whether to classify an observation (individual features) as being part of any of the available classes (individual database) is based on a computed score (MAP probability, distance measure, entropy). Three types of classifiers were studied:

- K-Nearest neighbors classifier

The K-Nearest neighbors classifier is based on the idea that an object is classified by a majority vote of its neighbors, with the object being assigned to the class most common amongst its k nearest neighbors. This is a common nonlinear classifier which results in a Voronoi tessellation of the feature space.

- MAP classifier

The Maximum a Posteriori classifier is based on the MAP probability of a class ω given an observation X

$$\hat{\omega} = \arg \max p(\omega|X). \quad (7)$$

In our work we assume that the observations can be modeled by a multivariate gaussian distribution given by

$$p(X, \mu, \Sigma) = \frac{1}{2\pi^{3/2}|\Sigma|^{1/2}} e^{-1/2(X-\mu)'\Sigma^{-1}(X-\mu)}. \quad (8)$$

In this framework the discriminant function to be maximized is given by

$$g_i(X) = \log p(X|\omega_i) + \log p(\omega_i) \quad (9)$$

$$g_i(X) = -\frac{1}{2} \log |\Sigma_i| - \frac{1}{2} (X - \mu_i)' \Sigma_i^{-1} (X - \mu_i) + \log p(\omega_i),$$

where μ_i and Σ_i are maximum likelihood estimates of the mean and covariance matrices of the pdf of class i , based on the training data; $p(\omega_i) = 1/N$, being N the number of individuals in the database.

- Minimum entropy distance classifier

As it was described before, the underlying observation model for each sample is described by a Rayleigh parameter (reflectivity). The approximated probability density function (PDFs) generated using this Rayleigh parameter can be compared with the other PDFs in the database (see Fig.9).

Conformity tests using the PDF for a given individual (testing distribution) and the remaining PDFs from the database (training distributions) were performed in order to assess which distribution better represents the observed one.

Considering the Kolmogorov-Smirnov conformity statistical test, $P_e = 1 - P_{H_0}$ is the probability of rejecting the null hypothesis, H_0 , which is the hypothesis of the data have been generated by any of the distributions from the database. Here, $P_{H_0} = Q_{KS}(\lambda)$, $Q_{KS}(\lambda) = 2 \sum_{j=1}^{\infty} (-1)^{j-1} e^{-2j^2\lambda^2}$, $\lambda = (\sqrt{N} + 0.12 + \frac{0.11}{\sqrt{N}}) D$, N is the number of data points and $D = \max |c(n) - ch(n)|$, where $c(n)$ and $ch(n)$ are the cumulative probability functions of the testing and training distributions.

The Kullback-Leibler entropy distance is given by, $d = \sum_n p(n) \log(\frac{p(n)}{h(n)})$. Here, $p(n)$ is the training distribution and $h(n)$ is the histogram of the observed (testing) sample.

5 RESULTS AND DISCUSSION

The performance of the classifiers was tested through 2 experiments and the result is summarized in Table 1. In the first experiment, 60 samples from one thyroid lobe were used as training data and 30 samples from the same lobe were used as testing data. The second experiment uses training data from one thyroid lobe (60 samples) and testing data from the opposite lobe (30 samples). Regarding the k-nearest neighbor and the MAP classifiers, tests were performed considering (i) all the features available,

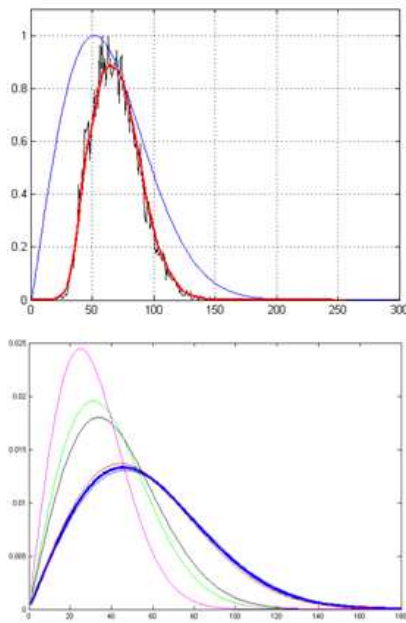


Figure 9: The histogram of an observed sample can be approximated by a Rayleigh distribution with an estimated parameter which accounts for the acoustic impedance of the sample tissue. This distribution can be compared with the others in the database and entropy distance measures can be computed.

Table 1: Performance of the classifiers (k-nNeigh, MAP, SmirKol, KullLeib) for two different data samples. Results achieved with the leave-one-out method are also shown.

Classifier	Identification Rate		
	Features	Exp.1	Exp.2
k-nNeigh	All	0.5000	0.2667
	PCA	0.5667	0.1667
	Radon+Wav.	0.4333	0.1667
MAP	All	0.2000	0.2000
	PCA	0.9000	0.7000
	Radon+Wav.	0.7000	0.3667
SmirKol kullLeib	Rayl	0.7000	0.1667
	Rayl	0.7000	0.2000
Leave1out	PCA	0.8778	0.9167

(ii) only the ones corresponding to the Radon transform and wavelets, which account for texture information, and (iii) the PCA derived features. The conformity tests (Kolmogorov-Smirnov, Kullback-Leibler) consider only the Rayleigh parameter (acoustic impedance or reflectivity) as describing each sample.

The best performance is achieved with the MAP classifier using the PCA derived features, with high correct identification rates for both experiments (ID rate for Exp.1 = 0.9000 and for Exp.2 = 0.7000). The ID rates obtained with the textural features

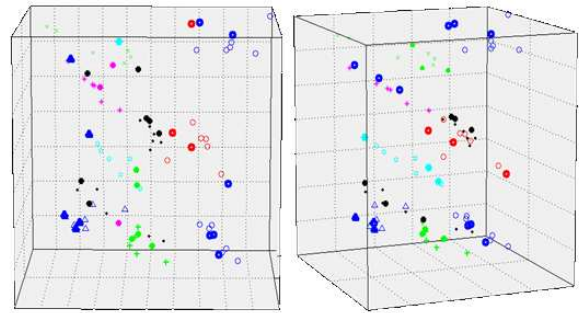


Figure 10: Performance of the classifiers from the feature space point of view. (Left) k-nearest neighbors classifier, (Right) MAP classifier. For each feature space, the true labels are plotted together with the classifier labels, represented in bold

(Radon+Wav.) and the MAP classifier were reasonably high, which allows to conclude that texture information is in fact relevant for tissue characterization and differentiation. Textural features have already been shown to be relevant in a similar context (SSST03a).

Fig.10 shows the comparison between the performance of the classifiers from the feature space point of view. It is clearly visible several misclassifications obtained with the k-nearest neighbors classifier. It is clear both from Fig.10 and Table 1 that the MAP classifier outperforms the k-nearest neighbors classifier.

A good performance is also achieved with the entropy distance classifiers (KullLeib and SmiKol) for the first data set (Exp.1). This suggests that the acoustic impedance of the thyroid tissue (which is the only parameter used by these two classifiers) is indeed a good parameter for discriminating between thyroids and thus individuals. The poor performance of these classifiers when using the second data set suggests that the echo-morphology varies significantly from one thyroid lobe to the other.

Another estimate of the accuracy of the classifier uses the leave-one-out method. In this case, all but one sample from each lobe (Exp.1) or from both lobes (Exp.2) were used, thus using a larger training data set. Here, the MAP classifier was used because it was the one which achieved better results in the aforementioned experiment. Again, considering Table 1 it is observed a good performance of the classifier, in which the classifier even outperforms for Exp.2. This suggests that the number of samples in the database significantly affects the performance of the classifiers.

6 CONCLUSIONS

Computer derived features from 2D ultrasound images of the thyroid glands were used as part of a prototype biometric system. These features are related to the acoustic impedance, texture and morphology of the thyroid tissue.

Good results were achieved with the MAP classifier, when using the three most discriminant features, computed by PCA. Moreover, reasonably high identification rates were also achieved with the entropy distance classifiers, suggesting that the acoustic impedance, or reflectivity, of the tissues is a relevant feature to discriminate between individuals. Analysis of thyroid echo-morphology should be further exploited because it appears to be very useful not only as a (soft) biometric system but also as a diagnostic tool.

Preliminary results, using only 9 parameters extracted from ultrasound images, are encouraging. Further studies, involving larger data sets (more individuals and more samples), as well as observations taken from multiple sessions along distinct time instants, are required to better establish the accuracy of this new biometric modality.

REFERENCES

- J. Abbot and F. Thurstone. Acoustic speckle: Theory and experimental analysis. *Ultrasound Imaging*, 1:303–324, 1979.
- C. Burckhardt. Speckle in ultrasound b-mode scans. *IEEE Transactions on Sonics and Ultrasonics*, SU-25(1):1–6, January 1978.
- Stephen Boyd and Lieven Vandenbergh. *Convex Optimization*. Cambridge University Press, 2004.
- Y. Boykov, O. Veksler, and R. Zabih. Fast approximate energy minimization via graph cuts. *IEEE Trans. Pattern Anal. Mach. Intell.*, 23(11):1222–1239, 2001.
- S. Catherine, L. Maria, A. Aristides, and V. Lambros. Quantitative image analysis in sonograms of the thyroid gland. *Nuclear Instruments and Methods in Physics Research A*, 569:606–609, December 2006.
- J. Dias, T. Silva, and J. Leitão. Adaptive restoration of speckled SAR images using a compound random markov field. In *Proceedings IEEE International Conference on Image Processing, Vol. II*, pages 79–83, Chicago, USA, October 1998. IEEE.
- R. M. Haralick, Dinstein, and K. Shanmugam. Textural features for image classification. *IEEE Transactions on Systems, Man, and Cybernetics*, SMC-3:610–621, November 1973.
- V. Kolmogorov and R. Zabih. What energy functions can be minimized via graph cuts? *IEEE Trans. Pattern Anal. Mach. Intell.*, 26(2):147–159, 2004.
- Guy Mailloux, Michel Bertrand, Robert Stampfler, and Serge Ethier. Computer analysis of echographic textures in hashimoto disease of the thyroid. *Journal of Clinical Ultrasound*, 14(7):521–527, 1986.
- O. V. Michailovich and A. Tannenbaum. Despeckling of medical ultrasound images. *IEEE Transactions on Ultrasonics, Ferroelectrics and Frequency Control*, 53(1):64–78, 2006.
- Salil Prabhakar, Josef Kittler, Davide Maltoni, Lawrence O’Gorman, and Tieniu Tan. Introduction to the special issue on biometrics: Progress and directions. *IEEE Trans. Pattern Anal. Mach. Intell.*, 29(4):513–516, 2007.
- M.A. Savelonas, D.K. Iakovidis, N. Dimitropoulos, and D. Maroulis. Computational characterization of thyroid tissue in the radon domain. *Computer-Based Medical Systems, 2007. CBMS ’07. Twentieth IEEE International Symposium on*, pages 189–192, June 2007.
- Daniel Smutek, Radim Sara, Petr Sucharda, and Ludvik Tesar. Different types of image texture features in ultrasound of patients with lymphocytic thyroiditis. In *ISICT ’03: Proceedings of the 1st international symposium on Information and communication technologies*, pages 100–102. Trinity College Dublin, 2003.
- Daniel Smutek, Radim Sara, Petr Sucharda, and Ludvik Tesar. Image texture analysis of sonograms in chronic inflammations of thyroid gland. *Ultrasound in Medicine and Biology*, 29:1531–1543(13), November 2003.
- José Seabra, João Xavier, and João Sanches. Convex ultrasound image reconstruction with log-euclidean priors. In *In Proc. of the Engineering in Medicine and Biology Conference*, Vancouver, Canada, 2008.
- Tortora Gerard J Tortora, Gerard J. (Gerard Joseph). Principles of anatomy and physiology, 2000.
- C. M. van Bommel, L. Spreeuwiers, M.A. Viergever, and W.J. Niessen. Level-set based carotid artery segmentation for stenosis grading. In *MICCAI ’02: Proceedings of the 5th International Conference on Medical Image Computing and Computer-Assisted Intervention-Part II*, pages 36–43, London, UK, 2002. Springer-Verlag.
- C. Xu and J.L. Prince. Snakes, shapes, and gradient vector flow. *IEEE Transactions on Image Processing*, 7(3), March 1998.